Available online at www.sciencedirect.com
SCIENCE DIRECT®
Journal of Magnetic Resonance 174 (2005) 200–208
JMR Journal of Magnetic Resonance
www.elsevier.com/locate/jmr

Side-chain H and C resonance assignment in protonated/partially deuterated proteins using an improved 3D ^{13}C-detected HCC–TOCSY

Kaifeng Hu *, Beat Vögeli, Konstantin Pervushin *

Laboratorium für Physikalische Chemie, Swiss Federal Institute of Technology, ETH-Hönggerberg, CH-8093 Zürich, Switzerland

Received 16 November 2004; revised 31 January 2005
Available online 10 March 2005

Abstract

We propose the use of ^{13}C-detected 3D HCC–TOCSY experiments for assignment of ^{1}H and ^{13}C resonances in protonated and partially deuterated proteins. The experiments extend 2D C-13-start and C-13-observe TOCSY type experiments proposed earlier [J. Biomol. NMR 26 (2) (2003) 167]. Introduction of the third ^{1}H dimension to 2D TOCSY: (i) reduces the peak overlap and (ii) increases the sensitivity per unit time, even for highly deuterated (>85%) protein samples, which makes this improved method an attractive tool for the side-chain H and C assignment of average sized proteins with natural isotope abundance as well as large partially deuterated proteins. The experiments are demonstrated with a 16 kDa ^{15}N, ^{13}C-labeled non-deuterated apo-CcmE and a 48 kDa uniformly ^{15}N,^{13}C-labeled and fractionally (~90%) deuterated dimeric sFkpA. It is predicted that this method should be suitable for the assignment of methyl ^{13}C and ^{1}H chemical shifts of methyl protonated, highly deuterated and ^{13}C-labeled proteins with even higher molecular weight.

Keywords: ^{13}C-detected NMR spectroscopy; Side-chain resonance assignment; apo-CcmE; sFkpA

1. Introduction

Recently, ^{13}C-detected NMR spectroscopy [2–5] has been proposed as an attractive alternative for studying large macromolecules [1,6]. Thus, two-dimensional (2D) ^{13}C-start and ^{13}C-observe TOCSY NMR experiments were successfully used for the assignment of side-chain aliphatic ^{13}C resonances in a completely deuterated protein with a molecular weight of 44 kDa [1] and measurement of a 'number of ^{13}C–^{13}C residual dipolar couplings [7]. As the protein size increases, the peak overlap becomes a significant problem, especially for monomeric proteins, which have a large number of residues. Simultaneous multiple-band-selective homonuclear ^{13}C- and ^{15}N-decoupling during both chemical shift evolution periods and signal acquisition can alleviate this problem to some extent by simplifying the multiplet patterns [8]. The introduction of a third chemical shift dimension in combination with extensive spin decoupling is expected to offer further reduction in peak overlap.

Here, we propose a pair of ^{1}H-start and ^{13}C-observe 3D HCC–TOCSY to facilitate assignment of the side-chain ^{1}H and ^{13}C resonances. Previously, 3D HCCH–TOCSY experiments were designed for protonated proteins in order to correlate the chemical shifts of H^i, C^i, and H^j, which is covalently bound to the adjacent non-frequency-labeled C^j [9,10]. Apparently, for partially deuterated proteins this experiment fails due to the low probability to find two protons simultaneously

* Corresponding authors. Fax: +41 1 632 1021 (K. Hu).
E-mail addresses: kaifeng.hu@bionmr.phys.chem.ethz.ch (K. Hu), kope@phys.chem.ethz.ch (K. Pervushin).

1090-7807/$ - see front matter © 2005 Elsevier Inc. All rights reserved.
doi:10.1016/j.jmr.2005.02.008

in a HCCH moiety. On the other hand, ^{13}C-detection relieves this requirement, thus enabling it to work at a very high level of proton dilutions. Comparing to the HMCM[CG]CBCA and amino acid-specific HMCM(CGCBCA)CO "out-and-back" experiments proposed by Kay and co-workers [11] for assignment of methyl groups in a 723 residue protein, we expect that the ^{13}C-detected "out-and-stay" HCC is better-suited and can be regarded as a general route for the assignment of methyl ^{13}C and ^{1}H chemical shifts for methyl protonated, highly deuterated, and ^{13}C-labeled proteins with high molecular weights [12,13]. A comparison to the original single-quantum ^{13}C-detected 3D HCC–TOCSY reported on a protonated 14 kDa protein alluded to potential application of ^{13}C-detected spectra [1,14]. The use of the ^{1}H–^{13}C multiple-quantum coherence during the chemical shift labeling period for the indirect ^{1}H and ^{13}C dimensions offers more favorable relaxation properties compared to the ^{13}C single-quantum coherence, as demonstrated for the ^{13}C′-detected 3D multiple-quantum-HACACO, 3D TROSY multiple-quantum-HN(CA)HA, and 4D TROSY multiple-quantum-HACANH experiments [15]. The HCC version proposed earlier [14] uses a single quantum non-constant time period for ^{1}H-labeling and $^{1}\mathrm{H} \rightarrow {}^{13}\mathrm{C}$ transfer. Subsequently, a constant time period labels ^{13}C. The new version employs the single quantum period only for 4 ms. Single quantum magnetization relaxes with a contribution proportional to the spectral density function at zero frequency, whereas during the multiple-quantum period the magnetization relaxes without such contribution [16]. Even though the new element is longer, a clear advantage can be expected, especially for large proteins. Another advantage of the proposed experiment is the possibility to use the resolved ^{13}C multiplet pattern along the directly acquired dimension in order to match resonances from different strips. In the construction of HCC–TOCSY, we pursued two alternative goals resulting in two complementary experiments. In the first experiment, referred to further on as IP-HCC–TOCSY, a clean, in-phase multiplet pattern in the directly acquired dimension is produced, facilitating sequential matching of 2D strips in the process of resonance assignment. In the second experiment, referred to as SE-HCC–TOCSY (SE stands for "sensitivity-enhanced"), the spectral sensitivity is maximized, which is achieved by relaxing the requirement of "in-phase" appearance of the resulting 3D spectra in the directly acquired dimension.

2. Materials and methods

Cytochrome *c* maturation heme chaperone protein E (CcmE) is a heme chaperone active in the cytochrome *c* maturation pathway of *Escherichia coli*, protecting the cell from premature activities of the highly reactive metalloorganic cofactor, which could cause oxidative damage. Uniformly ^{15}N-, ^{13}C-labeled apo-CcmE-His$_6$ (residues 30–159) was expressed and purified as described in [17]. The NMR sample contained 350 μl of 1 mM protein solution in 20 mM sodium phosphate buffer at pH 6.0 containing in addition 300 mM NaCl.

FkpA is a heat shock periplasmic peptidyl-prolyl *cis*/*trans* isomerase (PPIase) with chaperone activity. ^{15}N-, ^{13}C-, ^{2}H (90%)-labeled "shortened FkpA," sFkpA-His$_6$ (residues 10–224) was produced according to protocols described in [18]. The final ^{2}H, ^{15}N, ^{13}C-labeled NMR sample of the sFkpA protein is 1.2 mM in 20 mM Mes, pH 6.0, buffer with 20 mM NaCl.

NMR experiments were performed at 303 K on a Bruker AVANCE 500 and 600 MHz spectrometers equipped with a cryogenic Z-gradient DUL ^{13}C{H} probe, which is six times more sensitive than the conventional ^{1}H probe. NMR data were processed with the program NMRPipe [19]. Chemical shifts are reported relative to sodium 2,2-dimethyl-2-silapentane-5-sulfonate (DSS).

3. NMR experiments

Fig. 1 shows the experimental scheme of the 3D ^{13}C-detected HCC–TOCSY. The initial ^{1}H polarization is transferred to ^{13}C by an INEPT step generating ^{1}H–^{13}C multiple-quantum coherence during the chemical shift labeling period for the indirect $^{13}\mathrm{C}(t_1)$ and $^{1}\mathrm{H}(t_2)$ dimensions. In the IP experiment, τ_1 is set to $14\ \mathrm{ms} = 1/(2J_{\mathrm{CC}})$ in order to maximize the pure ^{13}C in-phase operator at the beginning of the FLOPSY-16 ^{13}C–^{13}C mixing period [20]. The pulse field gradients (PFG) are applied to select the in-phase operators before and after the TOCSY mixing. It should be noted that even with PFG based operator selection homonuclear ^{13}C zero-quantum terms insensitive to PFG can survive [21,22], resulting in distortion of the pure in-phase appearance of the crosspeaks [7,23]. Currently no efforts are made to prevent this. After a ^{13}C-read pulse, the NMR signal is detected during decoupling of ^{1}H or ^{2}H (for deuterated samples) spins. In the SE-HCC–TOCSY experiment, we aim to minimize relaxation and to preserve all magnetization transfer pathways. Therefore, τ_1 is set to much less than $14\ \mathrm{ms} = 1/(2J_{\mathrm{CC}})$ (e.g., 5 ms was used in the spectrum of Fig. 4). No gradients are applied before and after the mixing period to retain a superposition of in-phase and antiphase coherence significantly improving the signal-to-noise ratio. The product operator description of the coherence transfer pathway is given by diagrams (1) and (2) for the IP and the SE experiment, respectively:

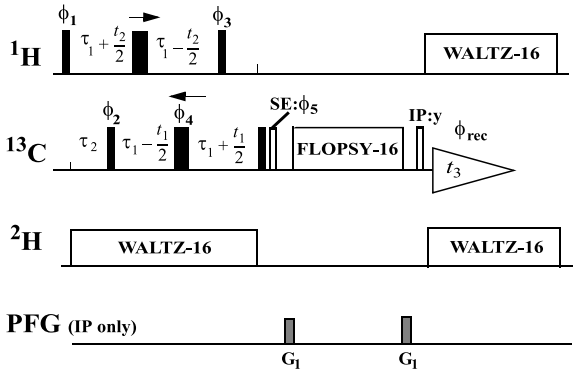

Fig. 1. Pulse sequence of ^{13}C-detected 3D-HCC–TOCSY, the radio-frequency pulses on ^{1}H, ^{13}C, and ^{2}H are applied at 2.5, 35, and 3.0 ppm, respectively. Narrow and wide bars indicate non-selective 90° and 180° pulses (black pulses are applied in both experiments; white pulses are only applied in the indicated experiment). ^{1}H- and ^{2}H-decoupling is achieved with WALTZ-16 [29] at a field strength around $\gamma B_1 = 2.5$ kHz. Unless indicated otherwise, all radio-frequency pulses are applied with phase x. The phase cycle is: $\phi_1 = \{x\}$; $\phi_2 = \{x, -x, x, -x, x, -x, x, -x\}$; $\phi_3 = \{y, y, y, y, -y, -y, -y, -y\}$; $\phi_4 = \{x, x, -x, -x\}$; $\phi_{rec} = \{x, -x, x, -x, -x, x, -x, x\}$. In the *IP experiment*: the delays are $\tau_1 = 1/(2J_{CC}) = 14$ ms, $\tau_2 = 1/(2J_{CH}) = 4$ ms. The FLOPSY-16 mixing time is 16.96 ms at $\gamma B_2 = 0.83$ kHz. Pulsed field gradients indicated on the line marked PFG are applied along the z-axis with duration of 0.9 ms and strength of 40 G/cm. Quadrature detection in the indirect ^{13}C (t_1) dimension and ^{1}H (t_2) dimension is achieved by the States–TPPI method [30] applied to the phases ϕ_1 and ϕ_2, respectively. In the *SE experiment*: the delays are τ_1 is set to smaller than $1/(2J_{CC}) = 14$ ms (depending on the relaxation properties of the multiple-quantum coherence), $\tau_2 = 1/(2J_{CH}) = 4$ ms. The FLOPSY-16 mixing time is shortened to 16.96/2 ms = 8.48 ms at $\gamma B_2 = 8.3$ kHz. Pulsed field gradients are not applied. A phase-sensitive spectrum in the indirect ^{13}C(t_1) dimension is obtained using the ECHO/ANTI-ECHO method by recording two FIDs for each t_1 value with $\phi_5 = \{x\}$ and $\phi_5 = \{-x\}$, respectively. Quadrature detection in the ^{1}H(t_2) dimension is achieved by the States–TPPI method applied to the phase ϕ_1.

$$\begin{aligned} &H_z^i \rightarrow -H_y^i \rightarrow 2H_x^i C_z^i \rightarrow -2H_x^i C_y^i[t_1,t_2] \rightarrow C_z^i \\ &\xrightarrow{\text{FLOPSY-16}} C_z^j \rightarrow C_x^j[t_3], \end{aligned} \tag{1}$$

$$\begin{aligned} &H_z^i \rightarrow -H_y^i \rightarrow 2H_x^i C_z^i \\ &\rightarrow -2H_x^i C_{\pm}^i \prod_m (a^m E + b^m i * 2C_z^m)[t_1,t_2] \\ &\rightarrow -C_{\pm}^i \prod_m (a^m[2\tau_1]E + b^m[2\tau_1] i * 2C_z^m) \\ &\xrightarrow{\text{FLOPSY-16}} C_{\pm}^j \prod_m (c^m E + d^m i * 2C_z^m) \\ &\rightarrow C_-^j \prod_l (c^l E + d^l i * 2C_z^l)[t_3], \end{aligned} \tag{2}$$

where H^i and C^i stand for the spins of the hydrogen and carbon atom of the bond i, from which the magnetization pathway starts. C^j stands for the directly detected carbon atom. C^m are spins involved in the J-coupled network of the spins C^i and C^j, and C^l are spin(s) bonded to the directly detected carbon C^j. Due to the coherence order selective mixing achieved by isotropic FLOPSY sequence [24], the "minus" operators evolving during t_1 are transferred exclusively to "minus" operators, which is used for signal acquisition. Quadrature detection is achieved by flipping "plus" and "minus" operators with a ^{13}C 180° pulse before TOCSY mixing. This results in the enhancement of sensitivity due to the coherence order selective transfer between adjacent ^{13}C spins. In addition, antiphase $2C_{\pm}^i C_z^j$ coherences developing during the t_1 period contribute to the C–C polarization transfer during isotropic mixing [25]. The mixture of in-phase or antiphase operators of C^i and C^j with respect to C^m and C^l is reflected by the time-dependent coefficients a^m, b^m and c^l, d^l with $\sqrt{(a^m)^2 + (b^m)^2} = 1$ and $\sqrt{(c^l)^2 + (d^l)^2} = 1$, respectively. In general, the splitting pattern becomes very complex due to the superposition of the in-phase and antiphase terms, as well as the different spin networks. Diagram (2) can be used to reconstruct the resonances of coupled ^{13}C spins by non-linear fitting of the theoretical line shapes to the experimental ones by variation of the parameters of c^l, d^l.

4. Results and discussion

As an example for the application to a protonated protein, Fig. 2 shows data from a spectrum of the 3D ^{13}C-detected IP-HCC–TOCSY measured on 16 kDa uniformly ^{15}N, ^{13}C-labeled apo-CcmE-His$_6$. Figs. 2A and B show H–C strips from the 3D ^{13}C-detected IP-HCC–TOCSY spectrum and HN strips from the 3D HNCACB spectrum for Val80 and Ile84, respectively. After the sequence-specific backbone assignment, $^{13}C^{\alpha}$ and $^{13}C^{\beta}$ chemical shifts can be aligned for identification of the side-chain spin systems. The complete spin system of Val80 can be clearly recognized. In the case of Ile84, all matching 2D H–C strips are found with the sole exception of the strip corresponding to γ^1 ^{13}C resonance. As an application to a large highly deuterated protein, a 3D IP-HCC–TOCSY was recorded on 0.8 mM uniformly ^{15}N-, ^{13}C-, ^{2}H (~90%)-labeled dimeric 48 kDa sFkpA-His$_6$. Figs. 3A and B show the 2D H–C strips from the 3D IP-HCC–TOCSY spectrum and HN strips from the 3D HNCACB spectrum of the complete spin systems of Leu123 and Lys154. As shown in Fig. 2, the $^{13}C^{\alpha}$ and $^{13}C^{\beta}$ chemical shifts can be aligned for identification of bonded H and C groups belonging to the same residue. The sign of the peaks in the H–C strips reports on the number of carbon neighbors helping the assignment. For example, the H–C strips for the β of Leu123 and the β, γ, and δ of Lys154 are opposite in sign to those in the other strips [1].

The high sensitivity of the SE version of the 3D ^{13}C-detected HCC–TOCSY was demonstrated on the 16 kDa uniformly ^{15}N, ^{13}C-labeled apo-CcmE-His$_6$ sample. Fig. 4A shows H–C strips from the 3D ^{13}C-detected SE-HCC–TOCSY spectrum for Ile84. Although

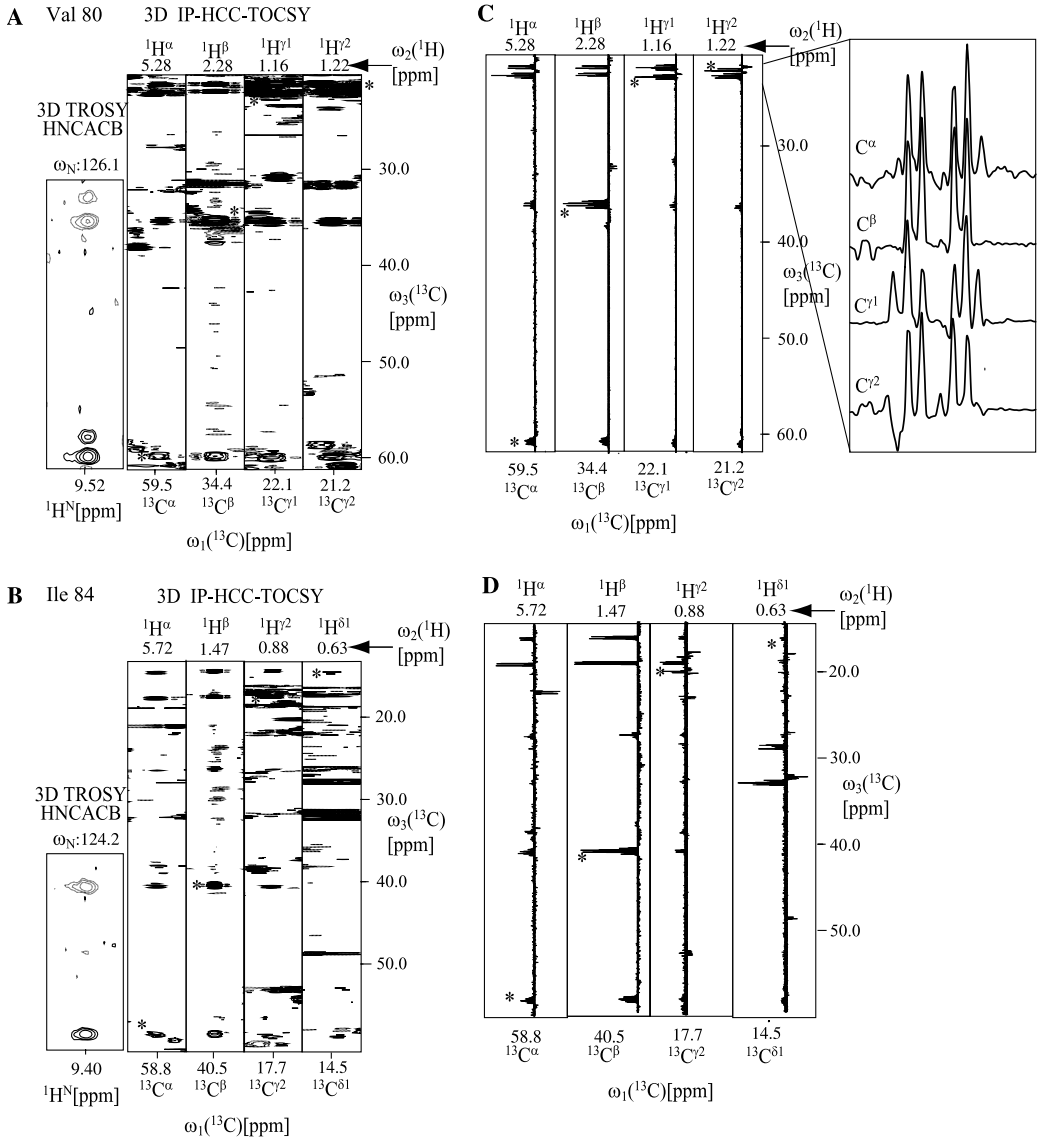

Fig. 2. H–C strips taken from the 3D ^{13}C-detected IP-HCC–TOCSY spectrum and HN strips taken from the 3D HNCACB spectrum for: (A) Val80 and (B) Ile84 of apo-CcmE-His$_6$. The corresponding indirect ^{13}C chemical shifts and their bonded ^{1}H chemical shifts are assigned and labeled for each strip. Diagonal peaks are marked with asterisks. $^{13}C^{\alpha}$ and $^{13}C^{\beta}$ chemical shifts are aligned to corresponding assigned signals in the 3D HNCACB. Slices taken along the direct ^{13}C dimension are shown in (C and D). The region of 20.5–22.5 ppm is magnified to present the resolved multiplets due to J_{CC} couplings. Alignment of the splitting pattern resolved at the high resolution obtained in the directly detected ^{13}C dimension, helps to confirm the assignment of the spin systems. The side-chain ^{1}H and ^{13}C chemical shifts of Val80 are completely assignable. The spin system of Ile84 can be identified without difficulty although the strip corresponding to $H^{\gamma 1}$–$C^{\gamma 1}$ is not visible. The experiment was performed at 600 MHz. $75(t_1)\times 24(t_2)\times 2048(t_3)$ complex points were accumulated, with $t_{1\max}$(indirect ^{13}C) = 9.93 ms, $t_{2\max}$(^{1}H) = 9.99 ms, and $t_{3\max}$(direct ^{13}C) = 168.7 ms, the interscan delay of 1 s and 56 scans per increment resulted in a total measurement time of 117 h. The time domain data were multiplied with a cosine function in all dimensions and zero-filled to $256\times 128\times 2048$ complex points.

the maximum of the components may shift by up to several Hertz due to the mixture of the in-phase and antiphase coherences and concomitant lineshape distortion, identification of spin systems is obtained with little difficulty and the $^{13}C^{\alpha}$ and $^{13}C^{\beta}$ chemical shifts can still be aligned with the corresponding signals from the HNCACB. Slices taken along the direct dimension are shown in Fig. 4B. An expansion shows the distorted multiplet patterns. As a comparison of Figs. 2D and 4D reveals, using approximately same measurement time as for IP-HCC–TOCSY, the SE version affords approximate eight times gain of signal-to-noise ratio. Shorter τ_1 and shorter TOSCY mixing time seems to play important role in sensitivity improvement for the non-deuterated protein sample, as shown in the comparison of Fig. 2 to Fig. 4. However, there is not an obvious experimental sensitivity factor gain achieved for the larger deuterated 44 kDa protein using the SE version com-

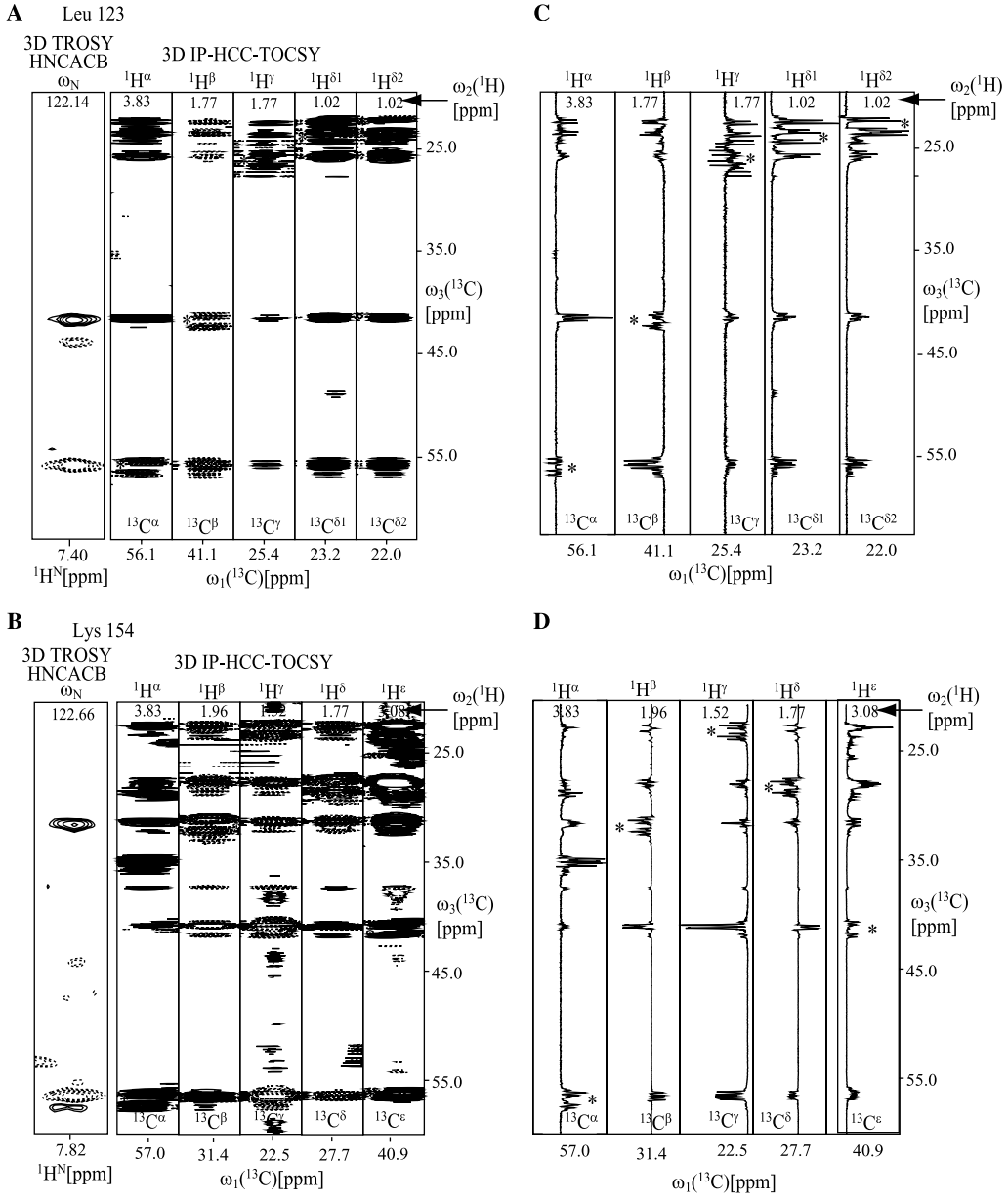

Fig. 3. H–C strips taken from the 3D ^{13}C-detected IP-HCC–TOCSY spectrum and HN strips taken from the 3D HNCACB spectrum for (A) Leu123 and (B) Lys154 of sFkpA-His$_6$. The corresponding indirect ^{13}C chemical shifts and their bonded ^{1}H chemical shifts are assigned and labeled for each strip. Diagonal peaks are marked with asterisks. $^{13}C^{\alpha}$ and $^{13}C^{\beta}$ chemical shift are aligned to their assignments in the 3D HNCACB. Slices taken along the direct ^{13}C dimension are shown in (C and D). The systems of both Leu123 and Lys154 are completely assigned. Broken lines indicate negative peaks. The peaks from the strips of $^{13}C^{\beta}$ of Leu123 and the $^{13}C^{\beta}$, $^{13}C^{\gamma}$, and $^{13}C^{\delta}$ of Lys154 are opposite in sign to the other strips, which further confirms the assignment of the spin systems. The experiment was performed at 500 MHz. $75(t_1)\times 24(t_2)\times 2048(t_3)$ complex points were accumulated, with $t_{1\max}$(indirect ^{13}C) = 11.93 ms, $t_{2\max}$(^{1}H) = 11.99 ms, and $t_{3\max}$(direct ^{13}C) = 203 ms, the interscan delay of 1 s and 56 scans per increment resulted in a total measurement time of 117 h. The time domain data were multiplied with a cosine function in all dimensions and zero-filled to $256\times 128\times 2048$ complex points.

pared to its IP counterpart (data not shown for the SE version). In the protonated protein sample, there is still a large amount of protons in the proximity of the H–C group, which in fact is a strong relaxation factor through H^p–H and H^p–C dipole–dipole coupling mechanism (here H^p is the proton in the proximity of the active H–C group). Therefore, for the non-deuterated protein sample, a shorter τ_1 and a shorter TOSCY mixing time can generally greatly improve the sensitivity. However, for the larger deuterated protein, we can assume that there are not too many protons in the proximity of the H–C group and consequently the relaxation due to H^p–H and H^p–C dipole–dipole coupling could be negligible, thus further shortening the τ_1 and TOSCY mixing time cannot bring an obvious sensitivity gain.

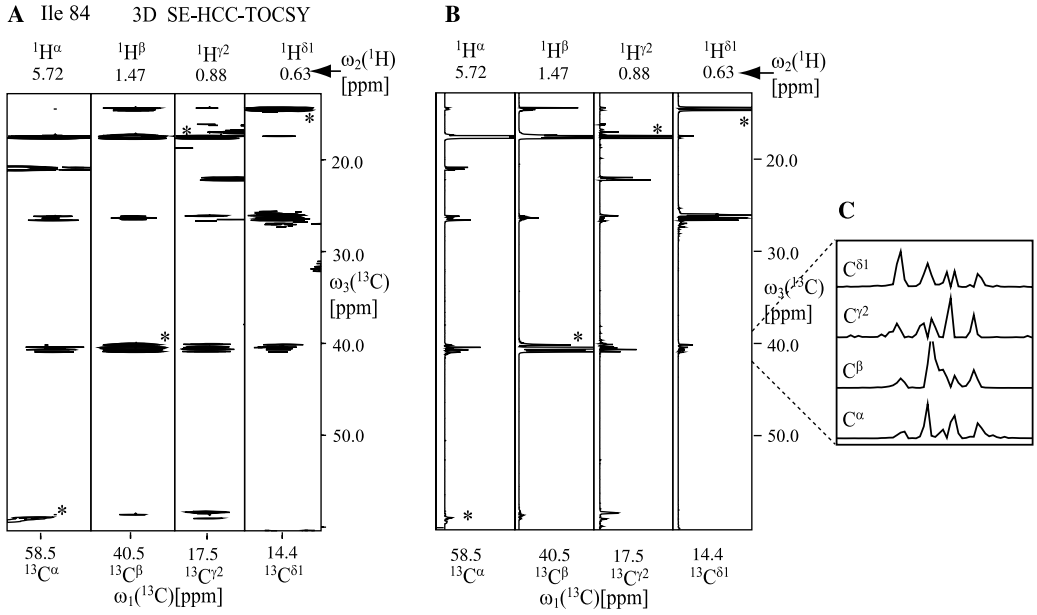

Fig. 4. (A) H–C strips taken from the 3D ^{13}C-detected SE-HCC–TOCSY spectrum for Ile84 of apo-CcmE-His$_6$. The corresponding indirect ^{13}C chemical shifts and their bonded ^{1}H chemical shifts are assigned and labeled for each strip. Diagonal peaks are marked with asterisks. Compared with Fig. 2B, the much cleaner spectrum demonstrates the significant gain in signal-to-noise ratio compared to the IP experiment, which facilitates the recognition of the spin systems. (B) Corresponding slices taken along the direct ^{13}C dimension. (C) Expanded regions showing the distorted lineshape of the peaks due to the mixture of in-phase and antiphase coherence. The experiment was performed at 600 MHz. $75(t_1)\times 26(t_2)\times 2048(t_3)$ complex points were accumulated, with $t_{1\max}$(indirect ^{13}C) = 9.93 ms, $t_{2\max}$ (^{1}H) = 10.82 ms, and $t_{3\max}$(direct ^{13}C) = 168.8 ms, the interscan delay of 1 s and 56 scans per increment resulted in a total measurement time of 126 h. The time domain data were multiplied with a cosine function in all dimensions and zero-filled to $256\times 128\times 2048$ complex points and Fourier transform was applied in power mode.

The identification of a spin system may be hampered by the non-uniform peak shapes recorded in the SE version. As can be inferred from diagram (2), each cross peak is a superposition of in-phase and antiphase components with particular phase values depending on the transfer pathway. The detected signals can be rewritten in the form of single transition operators:

$$\begin{aligned} &C^j_- \prod_l (c^l E + d^l i * 2C^l_z)[t_3] \\ &\quad = C^j_- \prod_l \{(c^l + id^l)(E/2 + C^l_z)[t_3] \\ &\qquad + (c^l - id^l)(E/2 - C^l_z)[t_3]\}. \end{aligned} \tag{3}$$

As can be seen from Eq. (3), each single transition component has its specific phase, which depends on c^l and d^l. Thus, in general, the superimposed peak cannot be phased to an absorptive pattern for all components. After Fourier transform a doublet peak can be written as:

$$\begin{aligned} S(\omega) = &\frac{AR_2\cos(\phi_1)}{R_2^2 + \left(\frac{J}{2} + \omega_0 - \omega\right)^2} + \frac{A\left(\frac{J}{2} + \omega_0 - \omega\right)\sin(\phi_1)}{R_2^2 + \left(\frac{J}{2} + \omega_0 - \omega\right)^2} \\ &+ \frac{AR_2\cos(\phi_2)}{R_2^2 + \left(-\frac{J}{2} + \omega_0 - \omega\right)^2} \\ &+ \frac{A\left(-\frac{J}{2} + \omega_0 - \omega\right)\sin(\phi_2)}{R_2^2 + \left(-\frac{J}{2} + \omega_0 - \omega\right)^2} + C \end{aligned} \tag{4}$$

with assumption of a Lorentzian lineshape for each peak component. Here, ω_0 is the chemical shift, A is an amplitude factor, R_2 is a uniform transverse relaxation rate (neglecting cross-correlated relaxation), ϕ_1 and ϕ_2 describe the phases for the two doublet components, respectively, J is the J_{CC} scalar coupling constant, and C is an arbitrary constant counting for the baseline level. A non-linear fit of Eq. (4) to the multiplet peak pattern may reveal the chemical shift together with all other parameters.

Fig. 5 shows slices through $C^{\gamma2}$ peaks of the spin system Ile84 of apo-CcmE-His$_6$. Although the shapes vary significantly, a non-linear fit yields chemical shift values differing only by up to 0.6 Hz. This deviation is smaller than the spectral resolution. Details on the fitting parameters are given in the figure caption. The power of this method strongly depends on the signal-to-noise ratio, the pattern complexity, the number of unknown parameters, and the performance of the fitting procedure. Using this procedure, one could even decompose overlapping peaks, although we designate the complete analysis of this problem to further other work. Clearly, the presented approach represents an attempt to effectively extract the relevant spectral information from the experiment maximizing spectral sensitivity. Probably a combination of IP and SE experiments would be necessary to unequivocally establish resonance frequencies of ^{13}C spins.

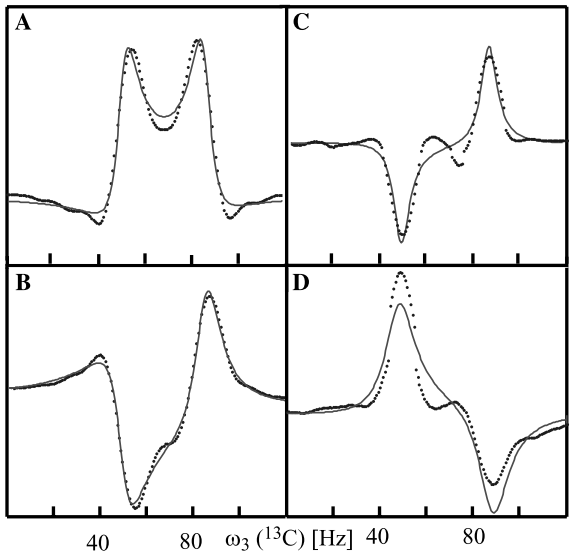

Fig. 5. Slices along the direct dimension through $C^{\gamma 2}$ peaks of the spin system Ile84 of apo-CcmE-His_6 (dotted lines) are taken from the 3D ^{13}C-detected SE-HCC–TOCSY spectrum. The corresponding indirect ^{13}C chemical shifts and their bonded ^{1}H chemical shifts are assigned to: (A) C^{α}, (B) C^{β}, (C) $C^{\gamma 2}$, and (D) $C^{\delta 1}$. The vertical scales are arbitrary. The solid lines represent the non-linear fit of Eq. (5) to the experimental line shapes using the program Matlab (The MathWorks, Inc.) in a seven-dimensional space comprising of: chemical shift ω_0, amplitude factor A, a uniform transverse relaxation rate R_2 (neglecting cross-correlated relaxation), the phases ϕ_1 and ϕ_2, the scalar coupling J, and an arbitrary baseline constant C. Source data are taken from 16.5 (set to 0 Hz in the plots above) to 17.3 ppm along the direct dimension. The values of the parameters obtained for ω_0, A, R_2, J, ϕ_1, ϕ_2, and C are: (A) 67.7, 970.6, 5.2, 35.8, 0.78, −0.90, −221.8; (B) 67.6, 1490.8, 6.8, 35.6, −0.40, −4.30, −221.7; (C) 68.2, 405.7, 7.8, 40.6, 2.93, −0.27, −211.4; (D) 68.2, 988.6, 4.2, 37.9, −0.06, −3.32, −220.0.

Besides reducing the overlap by introducing the ^{1}H dimension, an additional advantage of this ^{1}H-start 3D experiment is a significant reduction of the interscan delay from 2.5 s to less than 1 s in comparison to its ^{13}C-start 2D counterpart [1] due to faster equilibrium magnetization recovery of ^{1}H compared to ^{13}C in the ^{2}H–^{13}C moieties [26]. Neglecting transverse relaxation, theoretically, this improved ^{1}H-start and ^{13}C-observe 3D HCC–TOCSY can be expected to have comparable sensitivity per unit time to its ^{13}C-start and ^{13}C-observe 2D version as follows:

$$\Gamma = (S/N)_{\mathrm{HCC}}/(S/N)_{\mathrm{CC}} = \sqrt{\frac{T_1^{\mathrm{C}}}{T_1^{\mathrm{H}}}}\frac{\gamma_{\mathrm{H}}}{\gamma_{\mathrm{C}}}P, \tag{5}$$

where $(S/N)_{\mathrm{HCC}}$ and $(S/N)_{\mathrm{CC}}$ are signal-to-noise ratios in 3D HCC–TOCSY and 2D CC–TOCSY spectra, respectively. T_1^{C} and T_1^{H} are longitudinal relaxation times for ^{13}C and ^{1}H, with typical values for T_1^{C} of about 3–4 s and for T_1^{H} of 0.5–1 s. γ_{C} and γ_{H} are gyromagnetic ratios for ^{13}C and ^{1}H, and P indicates the proton level in the partially deuterated protein sample. For 90% deuterated protein samples, P is equal to 0.1 and the resulting Γ ranges from 0.7 to 1.1. Optimal sensitivity for the given protein size could be obtained by varying the deuteration level [27].

For the evaluation of the optimal deuteration level, we consider an exemplary configuration of $^{13}CX_2$, in which the magnetization starting on a proton is first transferred to its bonded carbon ^{13}C and both ^{1}H and ^{13}C chemical shifts are labeled in a MQ mode during the constant time period, and subsequently transferred to another $^{13}C(X_2)$ (by FLOPSY mixing during which relaxation is not considered), and the signal of the $^{13}C(X_2)$ is finally detected. Here, X stands for H or D. Following the method proposed by [28], we calculate the ratio of the signals of a partially deuterated sample to a fully protonated sample. The dipole–dipole coupling and chemical shift anisotropy (CSA) are assumed to be the only mechanisms for relaxation calculation and all cross-correlated relaxation terms are neglected. Relaxation due to dipole–dipole coupling with other protons in proximity is not taken into account in the analysis either. For proteins with large molecular size, only terms proportional to the spectral density function at the zero frequency, which make up the main contribution to the relaxation rate, are considered. As example, $\tau_1 = 4$ ms (^{1}H single quantum period, SQ_H), $\tau_2 = 24$ ms (^{1}H–^{13}C multiple-quantum period, MQ_HC) and the following expressions for relaxation rates are used:

$$R_{\mathrm{SQ\_H}} = R_{\mathrm{SQ\_H,CSA(H)}} + R_{\mathrm{SQ\_H,D(HC)}} + R_{\mathrm{SQ\_H,D(HX)}}, \tag{6}$$

$$R_{\mathrm{MQ\_HC}} = R_{\mathrm{MQ\_HC,CSA(H)}} + R_{\mathrm{MQ\_HC,CSA(C)}} + R_{\mathrm{MQ\_HC,D(CX)}} + R_{\mathrm{MQ\_HC,D(HX)}}. \tag{7}$$

Magnetization starting on D (for X = D) is not considered because it does not result in detectable signal in the HCC spectrum. For a partially deuterated protein sample, contributions to the signal are weighted with p^2 and $p(1-p)$ for CH_2 and CHD, respectively, where p is the protonation level. During detection, the average relaxation rate approximation is taken as [28]:

$$R_{\mathrm{SQ\_C}} = R_{\mathrm{SQ\_C,CSA(C)}} + 2(pR_{\mathrm{SQ\_C,D(CH)}} + (1-p)R_{\mathrm{SQ\_C,D(CD)}}). \tag{8}$$

Fig. 6A shows a 3D plot of the intensity gain of a partially deuterated sample over a fully protonated sample versus the correlation time τ_c and the protonation level p. Fig. 6B shows slices at $\tau_c = 5$, 20, and 40 ns. The optimal protonation level ranges from 0.15 to 0.20. This is close to the protonation level of the partially deuterated sFkpA protein (≈0.1) used for demonstration. It should also be noted that the relative gain of sensitivity for a partially deuterated sample over a purely protonated sample increases dramatically as the protein size becomes larger. For $\tau_c = 5$, the gain is around twofold. However, it can exceed 1000 times for larger size protein

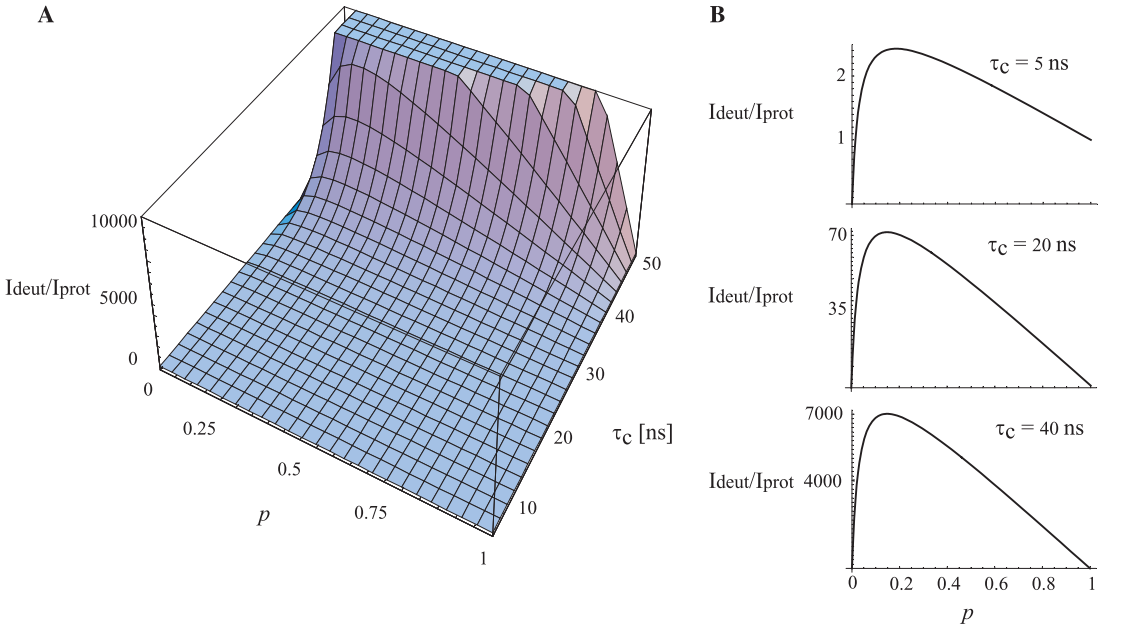

Fig. 6. (A) 3D plot of the intensity gain of a partially deuterated sample over a fully protonated sample versus the correlation time τ_c and the protonation level p. (B) Slices taken at $\tau_c = 5$, 20, and 40 ns from (A).

when τ_c is over 30 ns. During the FLOPSY mixing period, additional gain can also be expected due to the dipolar interactions between carbon and protons/deuterons. However, the detailed formalism of the relaxation during the FLOPSY mixing is very complicated and is out of the scope of the present work. The efficiency of the overall coherence transfer pathway depends on the H–C moieties with different configurations, such as CH, CH_2, and CH_3. The gain may be rather non-uniform for different H–C groups even at a certain deuteration level. Nonetheless, the model shows the strong advantage of deuteration, especially for large size protein samples.

In conclusion, the improved method presented here can serve as an attractive alternative to the standard H-detected side-chain H and C assignment strategies. High resolution and good sensitivity can overcome problems associated with ^{13}C-spectroscopy such as peak overlap. Especially for proteins with high molecular weight that requires partial deuteration, this method proved to be very useful as exemplified with the 48 kDa sFkpA. Because the recovery delay can be considerably shortened and magnetization starts on ^{1}H instead of ^{13}C, the experiment can yield comparable or higher sensitivity per unit experimental time. In addition to chemical shifts, the clear splitting pattern of the peaks along the directly detected ^{13}C dimension in IP type 3D ^{13}C-detected HCC–TOCSY can also be used to identify and confirm peak alignment. If the splitting pattern of the peaks is not of interest, the SE experiment can greatly increase the signal-to-noise ratio. More sophisticated homonuclear decoupling can further increase the signal-to-noise ratio [8]. The very high sensitivity indicates that the measurement time can be further shortened.

Acknowledgments

Financial support was obtained from a Swiss National Science Foundation grant to K.P. We thank Dr. Helena Kovacs for her help at the spectrometer at Bruker BioSpin AG and Dr. Fred Damberger for carefully reading the manuscript.

References

[1] A. Eletsky, O. Moreira, H. Kovacs, K. Pervushin, A novel strategy for the assignment of side-chain resonances in completely deuterated large proteins using C-13 spectroscopy, J. Biomol. NMR 26 (2) (2003) 167–179.
[2] A.A. Maudsley, L. Muller, R.R. Ernst, Cross-correlation of spin-decoupled NMR-spectra by heteronuclear 2-dimensional spectroscopy, J. Magn. Reson. 28 (3) (1977) 463–469.
[3] T.M. Chan, W.M. Westler, R.E. Santini, J.L. Markley, C-13 NMR sub-spectra of a protein based on the number of attached protons—ferredoxin from *Anabaena variabilis*, J. Am. Chem. Soc. 104 (14) (1982) 4008–4010.
[4] W.M. Westler, M. Kainosho, H. Nagao, N. Tomonaga, J.L. Markley, Two-dimensional NMR strategies for carbon carbon correlations and sequence-specific assignments in C-13 labeled proteins, J. Am. Chem. Soc. 110 (12) (1988) 4093–4095.
[5] B.H. Oh, W.M. Westler, P. Darba, J.L. Markley, Protein C-13 spin systems by a single two-dimensional nuclear magnetic-resonance experiment, Science 240 (4854) (1988) 908–911.
[6] W. Bermel, I. Bertini, I.C. Felli, R. Kummerle, R. Pierattelli, C-13 direct detection experiments on the paramagnetic oxidized

monomeric copper, zinc superoxide dismutase, J. Am. Chem. Soc. 125 (52) (2003) 16423–16429.
[7] B. Vögeli, H. Kovacs, K. Pervushin, Measurements of side-chain C-13–C-13 residual dipolar couplings in uniformly deuterated proteins, J. Am. Chem. Soc. 126 (8) (2004) 2414–2420.
[8] B. Vögeli, H. Kovacs, K. Pervushin, Simultaneous ^{1}H- or ^{2}H-, ^{15}N- and multiple-band-selective ^{13}C-decoupling during acquisition in 13C-detected experiments with proteins and oligonucleotides. J. Biomol. NMR. 31 (1) (2005) 1–9.
[9] A. Bax, G.M. Clore, A.M. Gronenborn, H-1–H-1 correlation via isotropic mixing of C-13 magnetization, a new 3-dimensional approach for assigning H-1 and C-13 spectra of C-13-enriched proteins, J. Magn. Reson. 88 (2) (1990) 425–431.
[10] E.T. Olejniczak, R.X. Xu, S.W. Fesik, A 4D-HCCH–TOCSY experiment for assigning the side-chain H-1-resonance and C-13-resonance of proteins, J. Biomol. NMR 2 (6) (1992) 655–659.
[11] V. Tugarinov, L.E. Kay, Ile, Leu, and Val methyl assignments of the 723-residue malate synthase G using a new labeling strategy and novel NMR methods, J. Am. Chem. Soc. 125 (45) (2003) 13868–13878.
[12] K.H. Gardner, L.E. Kay, Production and incorporation of N-15, C-13, H-2 (H-1-delta 1 methyl) isoleucine into proteins for multidimensional NMR studies, J. Am. Chem. Soc. 119 (32) (1997) 7599–7600.
[13] N.K. Goto, K.H. Gardner, G.A. Mueller, R.C. Willis, L.E. Kay, A robust and cost-effective method for the production of Val, Leu, Ile (delta 1) methyl-protonated N-15-, C-13-, H-2-labeled proteins, J. Biomol. NMR 13 (4) (1999) 369–374.
[14] Z. Serber, C. Richter, V. Dotsch, Carbon-detected NMR experiments to investigate structure and dynamics of biological macromolecules, Chembiochem 2 (4) (2001) 247–251.
[15] K.F. Hu, A. Eletsky, K. Pervushin, Backbone resonance assignment in large protonated proteins using a combination of new 3D TROSY-HN(CA)HA, 4D TROSY-HACANH and C-13-detected HACACO experiments, J. Biomol. NMR 26 (1) (2003) 69–77.
[16] G.V.T. Swapna, C.B. Rios, Z.G. Shang, G.T. Montelione, Application of multiple-quantum line narrowing with simultaneous H-1 and C-13 constant-time scalar-coupling evolution in PFG-HACANH and PFG-HACA(CO)NH triple-resonance experiments, J. Biomol. NMR 9 (1) (1997) 105–111.
[17] E. Enggist, L. Thony-Meyer, P. Guntert, K. Pervushin, NMR structure of the heme chaperone CcmE reveals a novel functional motif, Structure 10 (11) (2002) 1551–1557.
[18] K.F. Hu, A. Plückthun, K. Pervushin, Letter to the Editor: backbone H–N, N, C-alpha, C′ and C-beta chemical shift assignments and secondary structure of FkpA, a 245-residue peptidyl-prolyl cis/trans isomerase with chaperone activity, J. Biomol. NMR 28 (4) (2004) 405–406.
[19] F. Delaglio, S. Grzesiek, G.W. Vuister, G. Zhu, J. Pfeifer, A. Bax, NMRpipe—a multidimensional spectral processing system based on unix pipes, J. Biomol. NMR 6 (3) (1995) 277–293.
[20] M. Kadkhodaie, O. Rivas, M. Tan, A. Mohebbi, A.J. Shaka, Broad-band homonuclear cross polarization using flip-flop spectroscopy, J. Magn. Reson. 91 (2) (1991) 437–443.
[21] O.W. Sørensen, M. Rance, R.R. Ernst, Z-filters for purging phase-distorted or multiplet-distorted spectra, J. Magn. Reson. 56 (3) (1984) 527–534.
[22] L. Braunschweiler, R.R. Ernst, Coherence transfer by isotropic mixing—application to proton correlation spectroscopy, J. Magn. Reson. 53 (3) (1983) 521–528.
[23] F. Kramer, B. Luy, S.J. Glaser, Offset dependence of homonuclear Hartmann–Hahn transfer based on residual dipolar couplings in solution state NMR, Appl. Magn. Reson. 17 (2-3) (1999) 173–187.
[24] T. Parella, A complete set of novel 2D correlation NMR experiments based on heteronuclear *J*-cross polarization, J. Biomol. NMR 29 (1) (2004) 37–55.
[25] O. Zerbe, T. Szyperski, M. Ottiger, K. Wuthrich, Three-dimensional H-1-TOCSY-relayed CT-[C-13,H-1]-HMQC for aromatic spin system identification in uniformly C-13-labeled proteins, J. Biomol. NMR 7 (2) (1996) 99–106.
[26] K. Pervushin, B. Vögeli, A. Eletsky, Longitudinal H-1 relaxation optimization in TROSY NMR spectroscopy, J. Am. Chem. Soc. 124 (43) (2002) 12898–12902.
[27] G. Richter, M. Kelly, C. Krieger, Y.H. Yu, W. Bermel, G. Karlsson, A. Bacher, H. Oschkinat, NMR studies on the 46-kDa dimeric protein, 3,4-dihydroxy-2-butanone 4-phosphate synthase, using H-2, C-13, and N-15-labelling, Eur. J. Biochem. 261 (1) (1999) 57–65.
[28] D. Nietlispach, R.T. Clowes, R.W. Broadhurst, Y. Ito, J. Keeler, M. Kelly, J. Ashurst, H. Oschkinat, P.J. Domaille, E.D. Laue, An approach to the structure determination of larger proteins using triple resonance NMR experiments in conjunction with random fractional deuteration, J. Am. Chem. Soc. 118 (2) (1996) 407–415.
[29] A.J. Shaka, J. Keeler, R. Freeman, Evaluation of a new broadband decoupling sequence—Waltz-16, J. Magn. Reson. 53 (2) (1983) 313–340.
[30] D. Marion, A. Bax, Baseline correction of 2D FT NMR-spectra using a simple linear prediction extrapolation of the time-domain data, J. Magn. Reson. 83 (1) (1989) 205–211.